Competitive Binding of Cholesterol and Ergosterol to the Polyene Antibiotic Nystatin. A Fluorescence Study

Liana Silva,* Ana Coutinho,*† Alexander Fedorov,* and Manuel Prieto*
*CQFM, Instituto Superior Técnico, Lisbon, Portugal; and †DQB, Bloco C8, Faculdade de Ciências, Universidade de Lisboa, Lisbon, Portugal

ABSTRACT Competition studies between cholesterol and ergosterol were carried out to gain insight into the binding interactions between nystatin and these sterols. Lipid vesicles were prepared with mixtures of palmitoyloleoylphosphocholine/ergosterol/cholesterol, and both sterol molar ratio and total content were varied. The inhibitory effect of cholesterol toward the ergosterol ability to induce the formation of long-lived fluorescent antibiotic species was used to detect nystatin-cholesterol interactions. It was found that the key factor controlling nystatin photophysical properties in the ternary lipid mixtures was their ergosterol/cholesterol molar ratio and not their overall sterol content. Moreover, permeabilization studies showed that nystatin was able to form pores in all the mixed vesicles, but the initial rate of pore formation was also dependent on the ergosterol/cholesterol molar ratio. Our data show that ergosterol is displaced by competing cholesterol, indirectly confirming cholesterol's ability to coassemble with nystatin. The distinct spectroscopic properties emphasize the different molecular architecture adopted by nystatin-cholesterol and -ergosterol complexes, and therefore are relevant to understanding the interaction of the antibiotic with membranes.

INTRODUCTION

Polyene antibiotics, including nystatin (Nys) and amphotericin B (AmB), are clinically important as potent antifungal agents. The biological target for their action is the plasma membrane of the antibiotic-sensitive organisms, where they are believed to exert their function through the formation of barrel-like membrane-spanning ion channels. The preferential interaction of these antibiotics with fungal as compared to mammalian cells has often been correlated with their relatively higher affinity for ergosterol (Erg) than for cholesterol (Chol), respectively (1,2). However, the role of sterols in polyene antibiotics mechanism of action remains poorly understood. In an effort to characterize the species formed in each case, different spectroscopic techniques have been employed previously to measure changes undergone by these polyene antibiotics in the presence of sterols (1–3). Nevertheless, a direct demonstration that polyene antibiotics establish an interaction with sterols in lipid bilayers has been elusive for a long time (4).

Recently, we have shown that both Chol and Erg are able to promote the formation of Nys pores in the lipid bilayers that lead to the dissipation of a potassium gradient, i.e., an antibiotic active species. However, only in Erg/1-palmitoyl-2-oleoyl-*sn*-glycero-3-phosphocholine (POPC) but not in Chol/POPC vesicles the absorption and fluorescence properties of this polyene antibiotic varied significantly with the sterol content of the lipid vesicles. We proposed that the molecular architecture of the active antibiotic species was dependent upon the type of sterol included in the membrane, and that the detected spectroscopic changes resulted from the antibiotic-Erg aggregates being putatively more rigid and stable than the Chol ones (5).

To further elucidate this question, and in an effort to determine the relative affinities of this antibiotic for Chol and Erg, we carried out competition binding studies between the two sterols and Nys by exploiting the sensitivity of its fluorescence properties to the aggregation state of the antibiotic. It has been shown earlier that the antibiotic's mean fluorescence lifetime is capable of tracking changes in Nys oligomerization state in the lipid bilayers, either resulting solely from the self-association of the membrane-bound antibiotic molecules in gel-phase lipid vesicles (6) or from the formation of Erg-antibiotic complexes (5). Our results show that the Erg/Chol ratio and not the overall sterol content of the three-component Erg/Chol/POPC vesicles was the key factor controlling Erg's ability in inducing the formation of long-lived fluorescent antibiotic species. Furthermore, Nys ability to permeabilize the ternary lipid vesicles was also dependent on the Erg/Chol molar ratio. This supports the view that Chol and Erg compete for the binding of Nys, and that the photophysical properties and consequently the molecular structure of the channels formed are very different in each case.

MATERIALS AND METHODS

Materials

The polyene antibiotic Nys and Chol were obtained from Sigma (St. Louis, MO). POPC and 1-palmitoyl-2-stearoyl(11,12)dibromo-*sn*-glycero-3-phosphocholine (brPC) were purchased from Avanti Polar Lipids

Submitted September 30, 2005, and accepted for publication February 1, 2006.

Address reprint requests to Manuel Prieto, Centro de Química-Física Molecular, Instituto Superior Técnico, 1049-001 Lisbon, Portugal. Tel.: 351-218419219; Fax: 351-218464455; E-mail: prieto@alfa.ist.utl.pt.

0006-3495/06/05/3625/07 $2.00

doi: 10.1529/biophysj.105.075408

(St. Louis, MO). Erg was obtained from Fluka Chemika (St. Louis, MO); 1,6-diphenyl-1,3,5-hexatriene (DPH) and 1-(4-trimethylammoniumphenyl)-6-phenyl-1,3,5-hexatriene *p*-toluenesulfonate (TMA-DPH) were obtained from Molecular Probes (Eugene, OR). All organic solvents were Uvasol grade and were supplied by Merck (St. Louis, MO).

Lipid vesicles

Large unilamellar vesicles (LUV) (total lipid concentration ~1.4 mM) were prepared as described elsewhere (7). Briefly, a lipid film, after drying under vacuum overnight, was hydrated with the desired buffer solution (20 mM Hepes-NaOH (pH 7.4) with 150 mM NaCl and 1 mM EDTA) and vortex-mixed to produce multilamellar vesicles (MLV). The suspension was subjected to eight freeze-thaw cycles and then extruded through polycarbonate filters (400 and 100 nm pore size filter, four and 10 times, respectively). The lipid concentration was determined in triplicate by phosphorus analysis (8). Adequate volume of Nys stock solution (~1 mM in methanol) was added by injection to the lipid vesicles. All the samples were allowed to equilibrate for 30 min before the measurements.

Nystatin partitioning experiments

Partition coefficients of Nys were determined by a centrifugation method using brominated lipids (5,9). The total and free Nys concentrations were assayed by absorption spectrophotometry using $\varepsilon_{304} = 7.4 \times 10^4\ M^{-1}cm^{-1}$ (10). The mol-fraction partition coefficient, K_p, of Nys was calculated according to Santos et al. (11).

Binary phase diagram determination

MLV (total lipid concentration 0.2 mM) of Erg/POPC binary mixtures were prepared as described above. DPH was added at a probe to phospholipid molar ratio of 1:200 before lipid film formation. Steady-state fluorescence anisotropies ($\lambda_{exc} = 380$ nm and $\lambda_{em} = 428$ nm) were measured at different temperatures in 10 × 4 mm quartz cuvettes. The data were analyzed as described previously (12).

Nys activity assays

H^+/K^+ exchange assays across the membrane bilayer were carried out as described previously to indirectly evaluate the effect of Nys on the potassium permeability of the lipid vesicles (5). Briefly, the decrease in the fluorescence intensity of the entrapped pH sensitive pyranine was used to follow the acidification of the intravesicular space of the liposomes prepared with a variable lipid composition. The activity assays were started by submitting the liposomes to a transmembrane K^+ gradient of 3.3:1 $[K^+]_{in}$:$[K^+]_{out}$. After 120 s, Nys (5–25 μM final concentration) was added to the lipid suspension. Total dissipation of the K^+ gradient was obtained after the addition of the ionophore valinomycin to the liposomes after 300 s.

All the data were analyzed according to the formalism described in Coutinho et al. (5). The percentage of potassium gradient dissipation was calculated from:

$$\%\,K^+\ \text{dissipation} = \left(\frac{pH_{in}^{0} - pH_{in}^{300}}{pH_{in}^{0} - pH_{in}^{val}}\right) \times 100, \qquad (1)$$

where pH_{in}^{o} and pH_{in}^{300} are the pH inside the lipid vesicles at times $t = 0$ s and $t = 300$ s and $pH_{in}^{val}$is the pH obtained after the addition of valinomycin.

The apparent initial rate of pore formation by Nys in the liposomes, v_o, was determined from the initial slope of the function $p'(t)$, which is the apparent average number of pores per lipid vesicle that had been formed from $t = 0$ to t (13–15):

$$p'(t) = -1n\,R(t) = -\ln\left(\frac{pH_{in}(t) - pH_{in}^{300}}{pH_{in}^{0} - pH_{in}^{val}}\right), \qquad (2)$$

where $R(t)$ is the retention function of the liposome population and $pH_{in}(t)$ is the time course of the pH decrease of the inner vesicular space of the liposomes, which is followed by the variation of fluorescence intensity of pyranine.

Absorption and fluorescence measurements

Absorption spectra were measured at room temperature using a Jasco (Easton, MD) V-560 spectrophotometer and corrected for light-scattering artifacts by subtracting the respective blank sample. For steady-state fluorescence experiments an SLM-Aminco 8100 Series 2 spectrofluorometer (Jobin Yvon, Edison, NJ), with double excitation and emission monochromators and a 450 W xenon arc lamp was used. Nys fluorescence measurements were carried out in 0.5 × 0.5 cm quartz cuvettes using 320 and 410 nm as the excitation and emission wavelengths, respectively. Typically, excitation and emission slits of 4 nm were used. All the data were corrected for background intensities from antibiotic-free samples. Correction of excitation and emission spectra was performed using the software supplied by the manufacturer.

Steady-state fluorescence anisotropy measurements of TMA-DPH ($\lambda_{exc} = 355$ nm and $\lambda_{em} = 428$ nm) were carried out at a phospholipid molar ratio of 1:100. The time-correlated single-photon timing method was used to obtain the time-resolved fluorescence data. The instrumentation used was described in detail elsewhere (16). All the samples were excited at 320 nm and the emission (at 410 nm) was detected at the magic-angle (54.7°) relative to the vertically polarized excitation beam. The decays were analyzed using a sum of exponentials

$$I(t) = \sum_{i=1}^{n} \alpha_i \exp(-t/\tau_i), \qquad (3)$$

where α_i and τ_i are the normalized amplitude and lifetime of component i. The mean fluorescence lifetime was defined as,

$$\langle\tau\rangle = \sum \alpha_i \tau_i^2 \,/ \sum \alpha_i \tau_i. \qquad (4)$$

The adequacy of the multiexponential decay fit was judged by the reduced χ^2 value (values between 1.0 and 1.2 were accepted) with random distribution of residuals and autocorrelation of residuals. For all the systems four exponentials were always required to describe the fluorescence decay of Nys, in agreement with our previous studies (5).

RESULTS

Competition fluorescence studies between cholesterol and ergosterol for nystatin

The purpose of these experiments was to determine the relative affinity of the mammalian and fungal sterols, Chol and Erg, respectively, for the polyene antibiotic Nys by taking advantage of the sensitivity of its fluorescence properties to the oligomerization state of the membrane-bound antibiotic molecules. The first experiments were designed so that the total sterol mol fraction included in the liposomes was kept constant (10 mol % sterol), while the Erg/Chol molar ratio (E/C) of the ternary lipid mixtures was varied. This concentration was chosen because above this onset Erg is no longer the limiting reagent for mixed Erg-Nys complex formation (5). Therefore, it was anticipated that the eventual

competition between Chol and Erg for Nys binding should be maximal below this value. In the presence of 10 mol % Erg-containing POPC vesicles there was a pronounced increase in Nys's mean fluorescence lifetime from ~5 to 38 ns upon raising the overall antibiotic concentration (Fig. 1 *A*). The substitution of only one-fourth of Erg by Chol, i.e., upon preparing 7.5:2.5:90 Erg/Chol/POPC LUV, drastically reduced Nys's ability to form long-lived fluorescent antibiotic-Erg aggregates in the lipid bilayer. Further replacement of Erg by Chol, resulting in a ternary lipid mixture with an Erg/Chol ratio of 1, completely abolished this effect. The mean fluorescence lifetime of the antibiotic now becomes independent of its concentration, and is similar with the one observed for Nys interacting with sterol-free POPC LUV. In addition, the progressive substitution of Erg by Chol in the lipid bilayers also eliminated the alterations undergone by Nys fluorescence spectra, namely the appearance of a strong absorption at shorter wavelengths (~270–280 nm), concomitantly to the formation of the long-lived fluorescent antibiotic species (Fig. 1 *B*). These results cannot be solely ascribed to the reduction of the Erg content of the lipid vesicles because Nys's mean fluorescence lifetime still showed a reasonable increase with the antibiotic concentration used both in the presence of 5.0 and 7.5 mol % Erg-containing POPC LUV, as it is shown in Fig. 1 *A*.

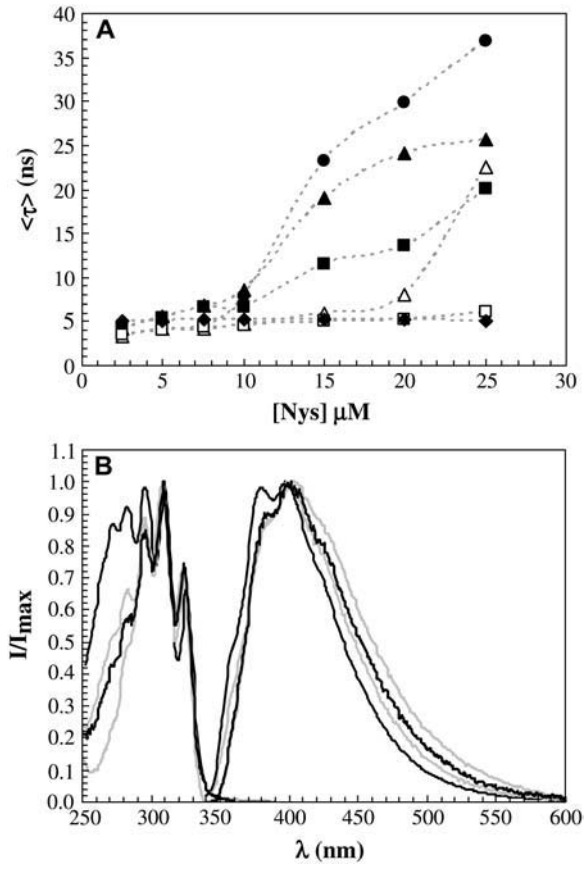

FIGURE 1 Effect of lipid vesicle composition on Nys spectroscopic properties. (*A*) Mean fluorescence lifetime, $\langle\tau\rangle$, of nystatin in POPC LUV containing (♦) 0 mol %, (■) 5 mol %, (▲) 7.5 mol %, and (●) 10 mol % ergosterol, or (△) 7.5:2.5 mol % Erg/Chol and (□) 5:5 mol % Erg/Chol, respectively. (*B*) Normalized excitation ($\lambda_{em} = 410$ nm) and emission ($\lambda_{exc} = 320$ nm) fluorescence spectra of 20 μM nystatin in the presence of POPC LUV with 10 mol % Erg (*thick black line*), 7.5:2.5 mol % Erg/Chol (*thick gray line*), 5:5 mol % Erg/Chol (*thin black line*) and 10 mol % Chol (*thin gray line*), respectively.

In a second set of experiments, the Erg content of the lipid vesicles was held constant and increasing amounts of Chol were added to the liposomes until reaching 30 mol % total sterol. As shown in Fig. 2, *A* and *B*, where Erg content was 7.5 and 20 mol %, respectively, the supplementation of the initial binary Erg/POPC mixtures with increasing amounts of Chol caused again the progressive disappearance of the long-lived fluorescent antibiotic species formed by Nys in the liposomes. The data further show that the key factor controlling the extent of formation of long-lived fluorescent antibiotic oligomers was the Erg/Chol ratio, and not the total sterol content (Fig. 2 *C*). For example, the addition of up to 25 μM Nys to 7.5:22.5:70 Erg/Chol/POPC (E/C = 1:3, *open squares*, Fig. 2 *A*) liposomes did not produce any change in the fluorescence emission decay kinetics of the antibiotic. However, when the same range of Nys concentrations interacted with 20:10:70 Erg/Chol/POPC LUV (E/C = 2:1, *solid squares*, Fig. 2 *B*) a small proportion of slow decaying fluorescent antibiotic species could still be detected.

To check if Nys was able to permeabilize the membrane of the different lipid vesicles driving the formation of pores that lead to the total dissipation of the imposed K^+ gradient, activity studies were carried out. It was observed that addition of the antibiotic to the vesicles lead to a complete dissipation of the gradient, independently of the sterol composition (Fig. 3 *A*). However, the initial rate of pore formation was again highly dependent on the Erg/Chol molar ratio (Fig. 3, *B* and *C*).

Physical properties of the lipid vesicles prepared with a variable sterol composition

Altogether, the data above strongly suggest that the changes undergone by Nys fluorescence emission decay kinetics result from specific interactions established between the antibiotic and the two sterols—Erg and Chol—incorporated in the lipid bilayers. However, changes in the bulk physical properties of the lipid vesicles upon varying their sterol content and composition could also indirectly contribute to this behavior, e.g., by controlling Nys partitioning toward the liposomes, and thus must also be explored.

To clarify this point, the ability of Chol and Erg in forcing the phospholipid acyl chains to adopt a significantly higher molecular order in bilayers of POPC/sterol prepared with high sterol content was first compared. To this end, we determined the partial binary phase diagram of POPC/Erg lipid mixtures using DPH as a fluorescent probe. The fluorescence emission anisotropy of DPH is very sensitive to

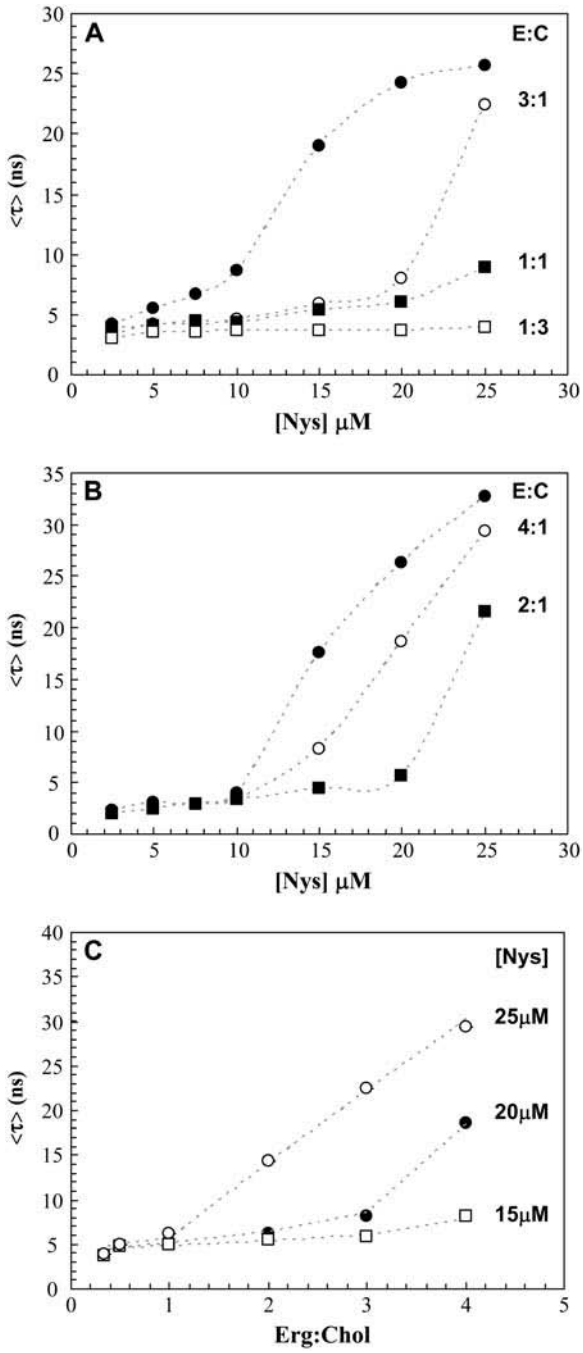

FIGURE 2 Ergosterol/cholesterol molar ratio determines Nys photophysical properties. Mean fluorescence lifetime, $\langle\tau\rangle$, of nystatin in POPC LUV containing (*A*) (●) 7.5 mol % Erg, (○) 7.5:2.5 mol % Erg/Chol, (■) 7.5:7.5 mol % Erg/Chol, and (□) 7.5:22.5 mol % Erg/Chol, and (*B*) (●) 20 mol % Erg, (○) 20:5 mol % Erg/Chol, (■) 20:10 mol % Erg/Chol, respectively. (*C*) Influence of the Erg/Chol molar ratio (E:C) present in the lipid vesicles on the mean fluorescence lifetime, $\langle\tau\rangle$, of (□) 15 μM, (●) 20 μM, and (C) 25 μM nystatin, respectively.

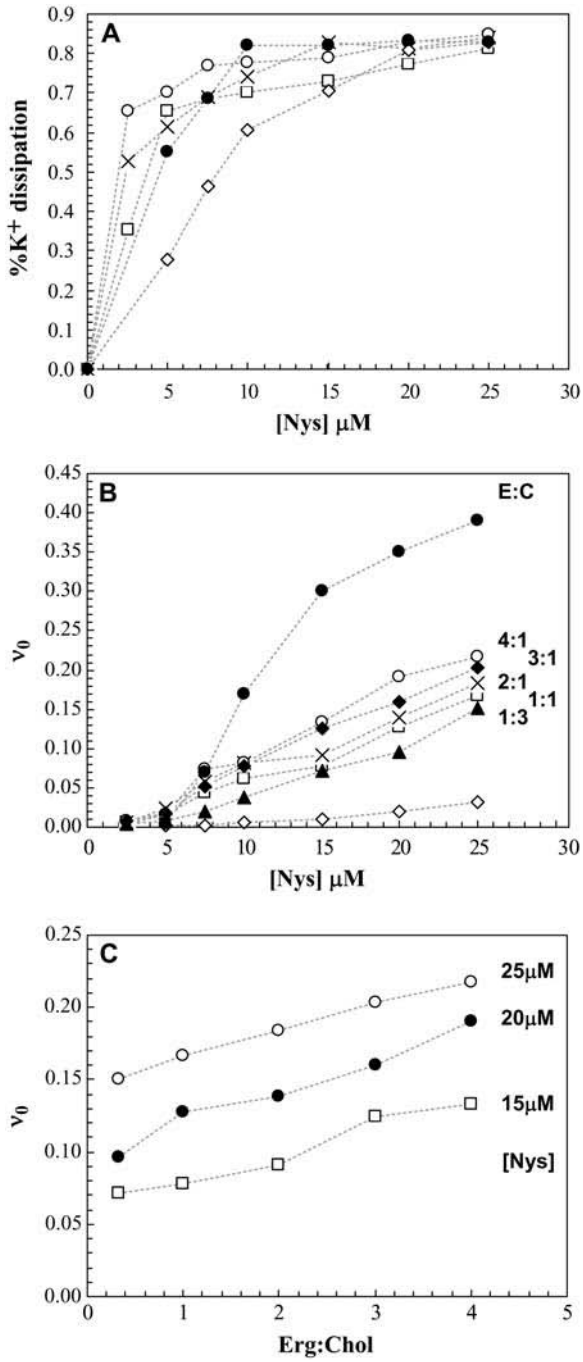

FIGURE 3 Erg/Chol molar ratio determines Nys ability to permeabilize lipid vesicles. (*A*) Percentage of transmembrane K^+ gradient dissipated by Nys 300 s after the beginning of each assay in POPC LUV containing (●) 10 mol % Erg, (◇) 10 mol % Chol, and (□) 5:5 mol %, (×) 10:5 mol %, and (○) 20:5 mol % Erg/Chol, respectively. (*B*) Apparent initial rate of pore formation, v_o, in POPC LUV containing (●) 10 mol % Erg, (◇) 10 mol % Chol, and (□) 5:5 mol %, (♦) 7.5:2.5 mol %, (×) 10:5 mol %, (○) 20:5 mol %, and (▲) 7.5:22.5 mol % Erg/Chol, respectively. (*C*) Influence of the Erg/Chol molar ratio (E:C) present in the lipid vesicles on the initial rate of pore formation, v_o, of (□) 15 μM, (●) 20 μM, and (○) 25 μM nystatin, respectively.

both the molecular order and dynamics of the phospholipid acyl chains (17), and its steady-state value can be used to monitor the appearance of a liquid-ordered phase, *l*o, in the lipid bilayers upon increasing their sterol mol fraction (12).

The results obtained for Erg/POPC binary mixtures are exemplified in Fig. 4 *A* for $T = 37°C$. Upon increasing Erg mol fraction, there was a progressive increase in the steady-state fluorescence emission anisotropy of DPH until ~40 mol % Erg was reached. The *l*d/*l*o phase boundaries of the binary system were identified as the two breakpoints detected in this plot at $X_{erg} = 13$ mol % and $X_{erg} = 41$ mol %, respectively (Fig. 3 *B*, *solid circles*). The phase diagram determined for POPC/Erg mixtures (Fig. 3 *B*, *solid circles*) is similar to the one previously published for POPC/Chol (Fig. 4 *B*, *open circles*) (12), except that at temperatures higher than 15°C the transition to a pure *l*o phase occurs at a lower Erg compared to Chol mol fractions. This suggests that Erg is a more effective promoter of the *l*o phase in POPC than Chol. It is interesting to note that Xu et al. (18) have also found that Erg promotes the formation of raft-like domains more strongly than Chol.

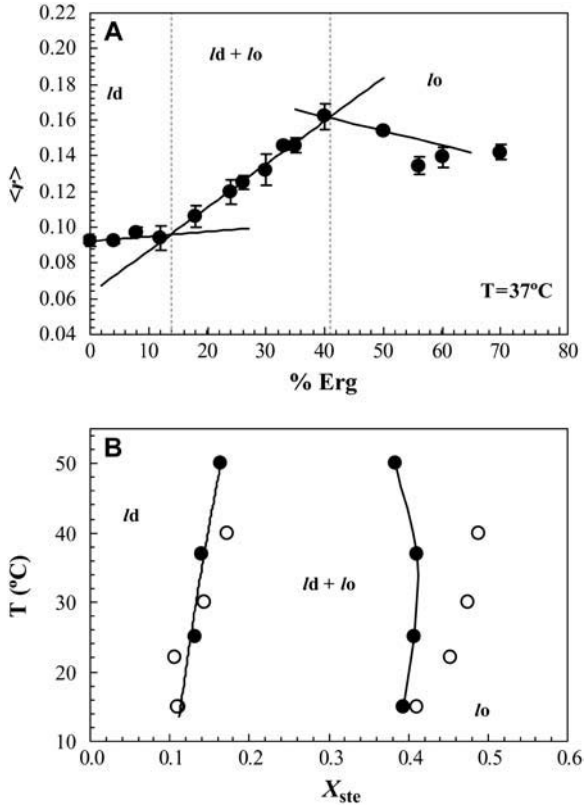

FIGURE 4 POPC/Erg binary phase diagram. (*A*) Determination of *l*d/*l*o phase coexistence boundaries for the binary lipid mixture POPC/ergosterol at 37°C using the steady-state emission fluorescence anisotropy of DPH, $\langle r \rangle$ ($\lambda_{exc} = 380$ nm and $\lambda_{em} = 428$ nm). The straight lines drawn through the experimental points distinguish the three regimes: *l*d phase, *l*d + *l*o coexistence, and *l*o phase for low, intermediate, and high ergosterol mol fractions, respectively. The vertical dashed lines were drawn only to guide the eye. (*B*) The partial binary phase diagram for POPC/ergosterol (●) was obtained from the intersections between the lines drawn at each temperature. The partial phase diagram previously obtained for POPC/cholesterol was also plotted (○) (12).

Secondly, we tested the possibility that the properties of the interfacial region of the lipid bilayers could be varying with the sterol content and Erg/Chol molar ratio used in the preparation of the liposomes, and thus indirectly modulating Nys fluorescence properties. Because the first step of Nys interaction with the lipid bilayers is expected to involve the adsorption of monomeric antibiotic molecules to the polar head region of the lipid membranes, we monitored the steady-state fluorescence emission anisotropy of TMA-DPH to explore this region of the lipid bilayer. TMA-DPH is a derivative of DPH with a cationic moiety attached to the para-position of one of the phenyl rings (19). Although DPH is known to be internalized into the hydrophobic core of the membrane, the amphipathic TMA-DPH is localized in the membrane bilayer with its positive charge localized at the lipid-water interface (20). As shown in Table 1, the steady-state fluorescence emission anisotropy of TMA-DPH was essentially independent of the Erg/Chol molar ratio or the total sterol content of the binary and ternary lipid mixtures studied, $\langle r \rangle \approx 0.22 \pm 0.01$.

Nystatin partitioning toward lipid vesicles prepared with a variable sterol composition

The previous result is in agreement with earlier findings showing that the partitioning behavior of Nys was not affected by the membrane sterol type nor content (0–30 mol %), always presenting a mol-fraction partition coefficient, $K_p \approx 1.5 \times 10^4$ toward the binary sterol/POPC lipid mixtures used (5). We further confirmed here that the use of LUV prepared with a three-component lipid mixture (Erg/Chol/POPC) did not change the partitioning equilibrium of Nys toward the LUV prepared (Table 1, $K_p \approx (1.4 \pm 0.2) \times 10^4$).

DISCUSSION

In this study, we addressed the question whether fluorescence spectroscopy could be used to indirectly detect the

TABLE 1 Influence of the lipid composition on the steady-state fluorescence emission anisotropy, $\langle r \rangle$, of TMA-DPH and nystatin partition coefficient, K_p, in sterol-containing POPC LUV

Mol percent ergosterol	Mol percent cholesterol	Total mol percent sterol	$\langle r \rangle$ ± 0.02	K_p (± 0.60 × 10^4)
2.5	2.5	5	0.21	–
5	5	10	–	1.58
7.5	2.5	10	–	1.45
7.5	7.5	15	0.21	–
7.5	22.5	30	0.23	1.59
10	5	15	0.21	1.05
10	10	20	0.20	–
15	–	15	0.21	–
20	–	20	0.21	1.67
20	5	25	0.22	1.52
20	10	30	0.22	–
30	–	30	0.22	1.40
–	20	20	–	1.42
–	30	30	0.22	1.31

formation of Nys-Chol aggregates in lipid membranes by a competition displacement assay. To this end, we have carried out time-resolved fluorescence measurements of Nys in the presence of ternary Erg/Chol/POPC lipid vesicles where both the total sterol content and Erg/Chol molar ratios was varied. The mean fluorescence lifetime of this polyene antibiotic has already proven to be a good reporter of Nys complexation with Erg in lipid bilayers (5). Our data show that the long-lived fluorescent antibiotic species, ascribed to the assembly of very rigid and compact Erg-antibiotic complexes in the lipid vesicles, progressively disappeared as the Chol concentration in the ternary lipid mixtures was increased, either by keeping constant the total sterol content (Fig. 1) or the Erg mol fraction (Fig. 2). Moreover, permeabilization studies showed that Nys was able to completely dissipate the K^+ gradient in all type of vesicles, thus confirming the formation of antibiotic active species independently of sterol composition. However, the initial rate of pore formation was dependent on the Erg/Chol molar ratio. Increasing Erg relatively to Chol sharply increased the initial rate of pore formation. In the ternary lipid vesicles, the presence of Erg always led to an initial gradient rate of dissipation higher as compared to the binary Chol/POPC vesicles, whereas small amounts of Chol had the opposite effect when compared to Erg/POPC vesicles.

It has been previously hypothesized that sterols may affect polyene antibiotics mode of action by two distinct mechanisms, which are not mutually exclusive: either through changes of the bulk physical properties of the lipid bilayer after modifications of its sterol content and/or via the establishment of specific antibiotic-sterol interactions. Discrimination between these two possibilities therefore requires characterization of the influence of sterols on membrane bilayer structural properties and on polyene antibiotics self-association. The eventual contribution of the first hypothesis to explain our time-resolved fluorescence data was ruled out because the partitioning behavior of Nys was not affected by the variable lipid composition (Erg/Chol/POPC ternary mixtures) used in the preparation of the LUV. Moreover, the steady-state fluorescence emission anisotropy of TMA-DPH failed to report any significant changes in the interfacial properties of these lipid vesicles upon varying their sterol content and composition. Also, the partial phase diagrams of Erg/ and Chol/POPC binary lipid mixtures were shown to be very similar (Fig. 4 *B*), only the first presenting a narrower *l*d + *l*o phase coexistence region as compared to the second one. Recently, Hsueh et al. (21) using deuterium nuclear magnetic resonance and differential scanning calorimetry studies have also shown that *l*o domains exist in liquid crystalline membranes containing Erg. Previous studies had already emphasized the comparable ability of Chol and Erg in inducing a more ordered packing of the phospholipid acyl chains in bilayers of phosphatidylcholines/sterol at high sterol content (22,23).

From the above, we conclude that the time-resolved fluorescence experiments and activity studies carried out in this study strongly support the view that Chol is competing with Erg for Nys binding in the membranes. Two nonmutually exclusive interpretations of the above data are possible: either Nys forms solely binary complexes with each type of sterol, or Erg can be progressively exchanged with Chol resulting in the formation of mixed ternary antibiotic-Erg-Chol complexes with probable variable antibiotic:Erg:Chol stoichiometries and aggregation numbers. In both cases, it is expected that the progressive displacement of Erg by Chol must induce a structural rearrangement in the aggregates, causing a decrease in the overall rigidity experienced by the polyene chains of Nys, and therefore abolishing their typical long mean fluorescence lifetime. Interestingly, Thewalt and co-workers (21) showed that in the presence of Erg the chain conformational freedom of 1,2-dipalmitoyl-*sn*-glycero-3-phosphocholine (DPPC) is lower when compared to the effect of Chol. Also, Urbina et al. (23) have shown that 30 mol % Erg orders the acyl chains of dimyristoylphosphatidylcholine more strongly than Chol. Thus, is also likely that Nys aggregates experience a higher rigidity in the presence of Erg. It should be stressed that excitonic coupling and formation of long-lived oligomers can only be explained by an increase in the packing that brings close together with a parallel orientation the transition moments of the chromophores (5). The differences observed for the initial rate of pore formation can be explained by the formation of channels with similar conductances but different lifetimes, as shown by Brutyan and McPhie (24). The stability of the channels is also a key element in the rate of permeabilization. Molecular modeling studies with AmB (25) have shown that the antibiotic channels were more stable in the presence of Erg-containing as compared to Chol-containing membranes. It is then possible that Erg increases the stability of Nys channels by increasing the rigidity of the aggregate structure.

Due to the complexity of the system studied, and lack of information about the homogeneity and stoichiometries of the simpler Nys-Erg and Nys-Chol binary complexes, dissociation constants for Nys-sterol interactions could not be calculated from the above data, preventing an evaluation of Nys-sterol affinities. Eventually, the performance of single-channel recording experiments with Nys might help to characterize the properties of the putative mixed Erg-Chol-antibiotic species formed in similar ternary lipid mixtures, like Brutyan and McPhie (24) and Matsumori et al. (26) did with AmB and AmB-sterol covalent conjugates, respectively.

CONCLUSIONS

In summary, our results show that Chol has the ability to abolish the formation of strongly fluorescent Nys-Erg complexes in sterol-containing POPC LUV. This effect stems from a direct competition between these two sterols for Nys binding, indirectly confirming Chol's ability to coassembly

with the antibiotic, and does not result from a change in the membrane structural properties due to a variation of their overall sterol content or the Erg/Chol molar ratio. To our knowledge this is the first study clearly showing a direct interaction between Nys and Chol. These results are relevant in the context of the characterization of the distinct steps involved in Nys mode of action at the molecular level, and emphasize the different spectroscopic properties presented by the mixed Nys-Chol and Nys-Erg assemblies formed in the lipid bilayers, giving insight to their distinct molecular architectures.

This work and research grants (BD/10029/2002 to L.S. and BPD/11488/2002 to A.F.) were supported by POCTI/Fundação para a Ciência e Tecnologia, Portugal.

REFERENCES

1. Bolard, J. 1986. How do the polyene macrolide antibiotics affect the cellular membrane properties? *Biochim. Biophys. Acta.* 864:257–304.
2. Hartsel, S. C., C. Hatch, and W. Ayenew. 1993. How does amphotericin B work? Studies on model membrane systems. *J. Liposome Res.* 3:377–408.
3. Fujii, G., J. E. Chang, T. Coley, and B. Steere. 1997. The formation of amphotericin B ion channels in lipid bilayers. *Biochemistry.* 36:4959–4968.
4. Dufourc, E. J., I. C. Smith, and H. C. Jarrel. 1984. Interaction of amphotericin B with membrane lipids as viewed by ^{2H}-NMR. *Biochim. Biophys. Acta.* 778:435–442.
5. Coutinho, A., L. Silva, A. Fedorov, and M. Prieto. 2004. Cholesterol and ergosterol influence nystatin surface aggregation: relation to pore formation. *Biophys. J.* 87:3264–3276.
6. Coutinho, A., and M. Prieto. 2003. Cooperative partition model of nystatin interaction with phospholipid vesicles. *Biophys. J.* 84:3061–3078.
7. Mayer, L. D., M. J. Hope, and P. R. Cullis. 1986. Vesicles of variable sizes produced by a rapid extrusion procedure. *Biochim. Biophys. Acta.* 858:161–168.
8. McClare, C. 1974. An accurate and convenient organic phosphorus assay. *Anal. Biochem.* 39:527–530.
9. Wimley, W. C., K. Hristova, A. S. Ladokhin, L. Silvestro, P. H. Axelsen, and S. H. Whyte. 1998. Folding of β-sheet membrane proteins: a hydrophobic hexapeptide model. *J. Mol. Biol.* 277:1091–1110.
10. Coutinho, A., and M. Prieto. 1995. Self-association of the polyene antibiotic nystatin in dipalmitoylphosphatidylcholine vesicles: a time-resolved fluorescence study. *Biophys. J.* 69:2541–2557.
11. Santos, N. C., M. Prieto, and M. A. R. B. Castanho. 2003. Quantifying molecular partition into model systems of biomembranes: an emphasis on optical spectroscopic methods. *Biochim. Biophys. Acta.* 1612: 123–135.
12. de Almeida, R. F. M., A. Fedorov, and M. Prieto. 2003. Sphingomyelin/phosphatidylcholine/cholesterol phase diagram: boundaries and composition of lipid rafts. *Biophys. J.* 85:2406–2416.
13. Schwarz, G., and C. H. Robert. 1990. Pore formation kinetics in membranes determined from the release of marker molecules out of liposomes or cells. *Biophys. J.* 58:577–583.
14. Schwarz, G., and C. H. Robert. 1992. Kinetics of pore-mediated release of marker molecules from liposomes or cells. *Biophys. Chem.* 42: 291–296.
15. Schwarz, G., and A. Arbuzova. 1995. Pore kinetics reflected in the dequenching of a lipid vesicle entrapped fluorescent dye. *Biochim. Biophys. Acta.* 1239:51–57.
16. Loura, L. M. S., A. Fedorov, and M. Prieto. 1996. Resonance energy transfer in a model system of membranes: application to gel and liquid crystalline phases. *Biophys. J.* 71:1823–1836.
17. Lentz, B. R. 1989. Membrane fluidity as detected by diphenylhexatriene probes. *Chem. Phys. Lipids.* 50:171–190.
18. Xu, X., R. Bittman, G. Duportail, D. Heissler, C. Vilcheze, and E. London. 2001. Effect of the structure of natural sterols and sphingolipids on the formation of ordered sphingolipid/sterol domains (rafts). *J. Biol. Chem.* 276:33540–33546.
19. Prendergast, F. G., R. P. Haugland, and P. J. Callahan. 1981. 1-[4-(Trimethylamino)phenyl]-6-phenylhexa-1,3,5-triene: synthesis, fluorescence properties, and use as a fluorescence probe of lipid bilayers. *Biochemistry.* 20:7333–7388.
20. Kaiser, R. D., and E. London. 1998. Location of diphenylhexatriene (DPH) and its derivatives within membranes: comparison of different fluorescence quenching analyses of membrane depth. *Biochemistry.* 37:8180–8190.
21. Hsueh, Y.-M., K. Gilbert, C. Trandum, M. Zuchermann, and J. Thewalt. 2005. The effect of ergosterol on dipalmitoylphosphocholine bilayers: a deuterium NMR and calorimetric study. *Biophys. J.* 88: 1799–1808.
22. Endress, E., H. Heller, H. Casalta, M. F. Brown, and T. M. Bayerl. 2002. Anisotropic motion and molecular dynamics of cholesterol, lanosterol, and ergosterol in lecithin bilayers studied by quasi-elastic neutron scattering. *Biochemistry.* 41:13078–13086.
23. Urbina, J. A., S. Pekerar, H. B. Le, J. Patterson, B. Montez, and E. Oldfield. 1995. Molecular order and dynamics of phosphatidylcholine bilayer membranes in the presence of cholesterol, ergosterol and lanosterol: a comparative study using $^{2H-}$, $^{13C-}$, and $^{31P-}$ NMR spectroscopy. *Biochim. Biophys. Acta.* 1238:163–176.
24. Brutyan, R. A., and P. McPhie. 1996. On the one-sided action of amphotericin B on lipid bilayer membranes. *J. Gen. Physiol.* 107: 69–78.
25. Baginski, M., H. Resat, and E. Borowski. 2002. Comparative molecular dynamics simulations of amphotericin B-cholesterol/ergosterol membrane channels. *Biochim. Biophys. Acta.* 1567:63–78.
26. Matsumori, N., N. Eiraku, S. Matsuoka, T. Oishi, M. Murata, T. Aoki, and T. Ide. 2004. An amphotericin B-ergosterol covalent conjugate with powerful membrane permeabilizing activity. *Chem. Biol.* 11: 673–679.